doi:10.3788/gzxb20154408.0823002

温度对单层有机电致发光器件电流平衡因子的影响

路飞平,刘晓斌,师应龙
(天水师范学院 物理系,甘肃 天水 741001)

摘 要:考虑有机薄膜中的陷阱,建立单层双极性有机发光器件的电学模型,研究了在不同的载流子迁移率和注入势垒条件下,器件工作温度对器件电流平衡因子的影响.研究表明:在低温工作区,当电子注入势垒和空穴注入势垒相等时,器件的电流平衡因子最大;在高温工作区,当电子迁移率大于空穴迁移率时,若电子注入势垒大于空穴注入势垒,器件的电流平衡因子最大,而当电子迁移率小于空穴迁移率时,情况恰好相反;当电子迁移率等于空穴迁移率时,电子注入势垒和空穴注入势垒相等时器件的电流平衡因子最大.此外,器件的电流平衡因子随着器件工作温度的升高而逐渐增大.可对设计高性能有机发光器件提供一定的理论参考.

关键词:电流平衡因子;工作温度;单层有机发光器件;数值研究;工作机理
中图分类号:TN383 **文献标识码**:A **文章编号**:1004-4213(2015)08-0823002-6

Influence of Working Temperature on the Current Balance Factor of Single Layer Organic Light-emitting Diodes

LU Fei-ping, LIU Xiao-bin, SHI Ying-long
(*Department of Physics, Tianshui Normal University, Tianshui, Gansu* 741001, *China*)

Abstract: The influence of the working temperature on the Current Balance Factor(CBF) value of the single layer Organic Light Emitting Diodes(OLEDs) was investigated by utilizing a numerical model of a bipolar single layer OLED with organic layer level traps. Results show that the largest CBF value can be achieved when the electron injection barrier (ϕ_n) is equal to the hole injection barrier (ϕ_p) in the lower working temperature region at any instance. In the higher working temperature region, the largest CBF can be achieved in the case of $\phi_n > \phi_p$ under the condition of electron mobility (μ_{0n}) larger than hole mobility (μ_{0p}), whereas the result for the case of $\mu_{0n} < \mu_{0p}$, is the opposite. When $\mu_{0n} = \mu_{0p}$, the largest CBF can be achieved in the case of $\phi_n = \phi_p$ in the entire region of the working temperature. In addition, the CBF value of the device increases as working temperature increasing. The results obtained in this paper can present an in-depth understanding of the OLEDs working mechanism.

Key words: Current balance factor; Working temperature; Single layer organic light-emitting diodes; Numerical study; Working mechanism
OCIS Codes: 230.3670; 000.6800; 240.0310

0 Introduction

Ease of fabrication, high efficiency, low cost, and compatibility with flexible substrates make Organic Light Emitting Diodes (OLEDs) attract a lot of research interests[1-4]. A larger Current Balance Factor (CBF), which is the ratio of the recombination current density and the total current density of the device, can guarantee a device to achieve high luminance and a long enough working lifetime at the same time. In order to improve the CBF of the devices, researchers always modify the interface of the electrode with a thin layer,

Foundation item: The National Natural Science Foundation of China (Nos. 11264033, 11464040), the Research Project of Graduate Teacher of Gansu Province (No. 2014B-079)

First author: LU Fei-ping (1980-), male, associate professor, Ph. D. degree, mainly focuses on the working mechanism of OLEDs. Email:lufp_sysu@163.com

Received: Mar. 26, 2015; **Accepted**: May. 15, 2015

such as inserting MnO[5], LiF[6], Al_2O_3[7], or $CsCO_3$[8] into the interface of the cathode/organic layer, or by inserting CuPc[9] or MoO_3[10] into the interface of the anode/organic layer, to adjust the injection ability of carriers. Malliaras et al. demonstrated that utilizing different cathode materials can change the injection ability of electrons, thereby changing the CBF of the devices, and also found that the external quantum efficiency of devices increases as working temperature increasing [11]. I-Min Chan et al. demonstrated that a very low turn-on voltage, along with significantly improved luminance and current density of the device can be achieved by depositing an ultra-thin layer of Nickel Oxide (NiO) on the Indium-Tin Oxide (ITO) anode to enhance hole injection in OLED, which can significantly improve the CBF value of the devices[12]. Markham et al. demonstrated a very high-efficiency green phosphorescence from a single layer dendrimer OLED formed by spin-coating, and attributed this exceptionally high quantum efficiency for a single-layer device to the excellent film forming properties and high photoluminescence quantum yield of the dendrimer blend and the efficient injection of charge into the emissive layer[13]. In previous paper, we ignored the level traps in organic layer, the influence of applied voltage on the CBF characteristic of single layer OLEDs was investigated by a numerical model of a bipolar single layer OLED with organic layer trap free and without doping[14]. However, in organic semiconductor thin films there exist, in general, shallow and deep level traps[15]. In this work, we extend the model to organic layer with level traps, and the influence of working temperature on the CBF characteristic of single layer OLEDs was investigated. The conditions for single layer OLEDs to obtain largest CBF were achieved at both lower and higher working temperature region, and the relationship between CBF of single layer OLEDs and the working temperature were also obtained. The results obtained in this paper can present an in-depth understanding of the working mechanism of OLED and help ones fabricate high efficiency OLEDs.

1 Model

In organic semiconductor thin films, there exist shallow and deep level traps. Shallow traps are distributed over the organic depth, and are the dominant, while deep level traps are located mainly at the metal/organic interface[16]. In our previous papers, we had developed a numerical model of a bipolar single layer OLED with organic layer traps free but without doping[14]. In this paper, we extend the model to organic layer with level traps. The density of shallow traps is exponentially distributed in energy as follows[17-18]

$$h(E_t)=\frac{H_t}{K_B Tl}e^{E_t/K_B Tl} \tag{1}$$

where E_t is the energy of traps respective to the energy of the Highest Occupied Molecular Orbit (HOMO) (for hole), and the energy of traps respective to the energy of the Lowest Unoccupied Molecular Orbit (LUMO) (for electron). $h(E_t)$ is the density of trap states per unit energy in the vicinity of trap energy E_t. l is the relative trap depth, which is defined as the ratio of the characteristic trap energy E_{tc} of trap distribution to thermal energy $K_B T$, that is $l=E_{tc}/K_B T$. H_t is the total density of traps, which can be obtained by the integration of the product of $h(E_t)$ and proper Fermi - Dirac distribution function over the trap energies in the range $[0, \infty]$. In organic semiconductors, the concentration of free carriers is generally much smaller than that of trapped carriers, and they are associated through following equations, for free holes and electrons[19]

$$p_f=N_0\left[\frac{\sin(\pi/l_p)}{H_t(\pi/l_p)}\right]p^{l_p} \tag{2}$$

$$n_f=N_0\left[\frac{\sin(\pi/l_n)}{H_t(\pi/l_n)}\right]n^{l_n} \tag{3}$$

where N_0 is the density of states of HOMO and LUMO of the organic material. p and n is the total hole and electron concentration in organic layers respectively, which is the sum of free and trapped carriers in organic layer[19]

$$p=p_f+p_t \tag{4}$$

$$n=n_f+n_t \tag{5}$$

The current density of device was only determined by the free carrier concentration, so the hole and electron current density equation in Ref. [14] should be changed as the following

$$J_p=q\mu_p p_f F-D_p q\frac{dp_f}{dx} \tag{6}$$

$$J_n=q\mu_n n_f F+D_n q\frac{dn_f}{dx} \tag{7}$$

The equations of the model are numerically solved by the Scharfetter-Gummel method[20-21].

2 Results and discussions

This section discusses the CBF of the OLEDs in three different conditions according to the relation of the electron and the hole mobility values.

2.1 $\mu_{0n}>\mu_{0p}$

Fig. 1 shows the relationship between working temperature and CBF value, the hole and electron concentration, and the electric field intensity distribution in the bulk of organic layer in the cases of electron injection barrier (ϕ_n) >, = and < hole injection barrier (φ_p) for a single layer OLED with electron mobility (μ_{0n}) larger than the hole mobility (μ_{0p}), where the parameters used are: $\mu_n = 1\times10^{-5}$ cm^2 • V^{-1} • s^{-1}, $\mu_p = 1\times10^{-6}$ cm^2 • V^{-1} • s^{-1}, $n_0 = p_0 = 1\times10^{21}$ cm^{-3}, $F_{n0} = F_{p0} = 5\times10^5$ V • cm^{-1}, $T = 300$ K, $V = 12$ V, $d = 100$ nm, $E_g = 3.0$ eV, $N_0 = 1\times10^{21}$, $l_n = l_p = 3.0$, $\varepsilon_r = 3$.

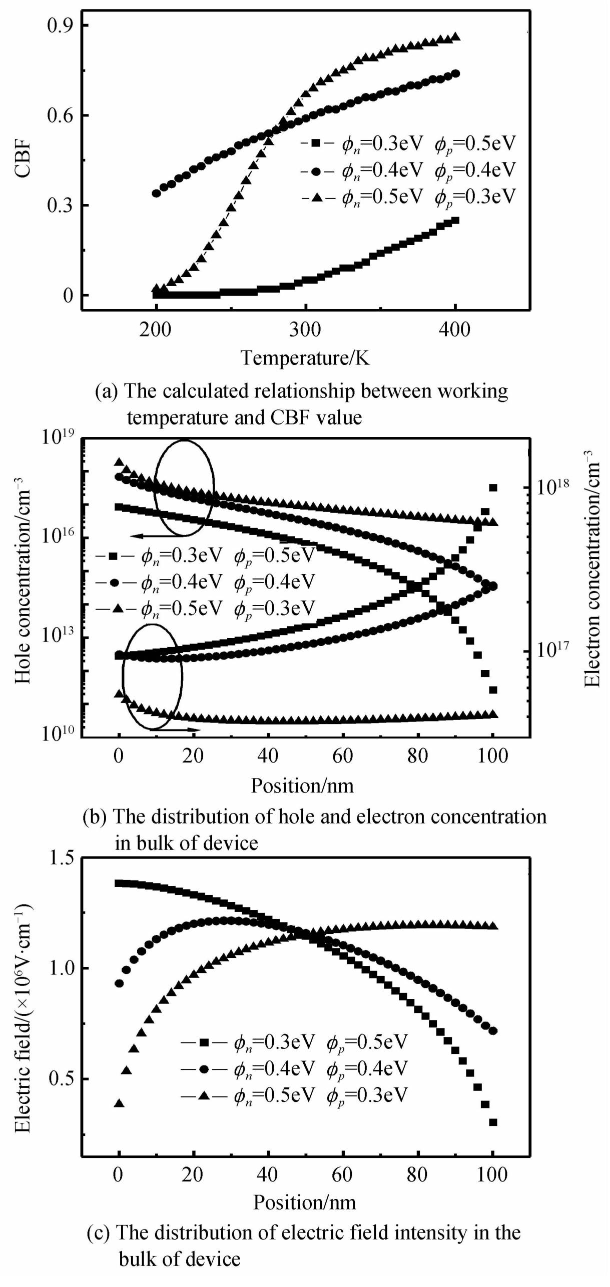

Fig. 1 The calculated results in the case of $\mu_{0n} > \mu_{0p}$

Under a lower working temperature, the thermionic emission current density at the interface of electrode/organic layer is small according to Eq. (14) in Ref. [14], the current density of device is mainly determined by the tunneling current, and in this case, few carriers can be injected into the organic layer comparing with the condition that the working temperature is higher. Because the number of injected carrier is little, carriers can transport into the organic film bulk with little accumulation at the interface of the electrode/organic, the electric field intensity at the interface of electrode/organic layer is nearly equal. In this case, the electron and the hole have nearly the same injection ability at the lower working temperature region when $\phi_n = \phi_p$, so devices have the largest recombination current and CBF compared with the cases of $\phi_n > \phi_p$ and $\phi_n < \phi_p$, as shown in Fig. 1(a).

As the working temperature increasing to a relative higher region, more carriers can be injected into the organic thin film comparing with the case of lower working temperature region, in this case, because of the low mobility of the organic film, some of the injected carriers will accumulate at the vicinity of the interface of electrode/organic (as shown in Fig. 1(b)). According to the Eqs. (14), (19) and (20) in Ref. [14], the numbers of injected holes are less than the number of injected electrons when $\phi_n < \phi_p$, as shown in Fig. 1(b). Meanwhile, holes accumulate at the vicinity of the interface of anode/organic because of their lower mobility compared with the electrons. The accumulated holes generate an inner electric field with an opposite direction to the applied electric field, leading to the interface electric field intensity being lower than the initial value ($=V/L$, where V is the applied voltage and L is the thickness of organic layer). The greater the accumulation at the vicinity of the anode/organic interface, the lower the interface electric field intensity at the vicinity of the anode/organic interface (as shown in Fig. 1(b) and 1(c)), in this case, the effective injection barrier is higher than the case of that carriers with lower accumulation at the vicinity of the anode/organic interface according to Eq. (15) in Ref. [14], thereby restraining the injection ability of the holes. Meanwhile, more electrons can be injected into organic layers because the injection barrier is lower; however, the injected electrons can easily transport from the interface into the organic bulk compared with holes because the electron mobility is larger than the hole. Ultimately, the accumulation of electrons at the vicinity of the cathode/organic interface is reduced. In this situation, the carriers injected from both electrodes are deeply imbalanced, as shown in Fig. 1(b). In this case, devices have the smallest CBF compared with the cases of $\phi_n = \phi_p$ and $\phi_n > \phi_p$ at the higher working temperature region.

When ϕ_n increases and ϕ_p decreases until $\phi_n = \phi_p$, the injection ability of the electron is reduced and the injection ability of the hole is improved. The injected electrons can easily transport from the interface into the organic bulk compared with holes because $\mu_{0n} > \mu_{0p}$. The hole accumulation at the vicinity of the anode/

organic interface is stronger than the electron accumulation at the vicinity of the cathode/organic interface (as shown in Fig. 1(b)), thereby leading to the imbalance of carrier injection from both electrodes. However, compared with the case $\phi_n < \phi_p$, the difference between the electrons injection ability and holes injection ability is reduced, so the CBF value is improved compared with $\phi_n < \phi_p$ at the higher working temperature region.

When ϕ_n continues to increase and ϕ_p continues to decrease until $\phi_n > \phi_p$, the electron injection ability is further reduced and the hole injection ability is further improved. The accumulation of carrier at the vicinity of the anode and cathode is different because of the different mobility of the holes and the electrons, resulting in different interface electric field intensities. Nevertheless, a case where in the carriers injected from both electrodes will be equal and may also exist, the difference between the electrons and holes injection ability is further reduced (as shown in Fig. 1(b)), so devices have the largest CBF compared with the cases of $\phi_n > \phi_p$ and $\phi_n < \phi_p$ at the higher working temperature region.

Moreover, the CBF value increases with increasing working temperature for all cases ($\phi_n > \phi_p$, $\phi_n = \phi_p$ and $\phi_n < \phi_p$), as shown in Fig. 1(a). Considering $\phi_n < \phi_p$ as an example, the carrier injection ability of an electron from the cathode is more effective than the hole from the anode under a given working temperature. Given the lower carrier mobility of organic layers, the number of carriers that accumulate at the vicinity of the electrode/organic interface will increase when more carriers are injected into the organic layer, thereby generating a stronger inner electric field. The interface electric field intensity at the cathode/organic becomes weaker (as shown in Fig. 1(c)), thereby reducing the injection ability of electrons, according to the Eqs. (14), (15), (19) and (20) in Ref. [14]. By contrast, the number of accumulated holes at the anode/organic interface is lower. The interface electric field intensity of the anode/organic interface may be larger than the cathode/organic interface. This difference results in the rate of increment of the hole injection ability being larger than the rate of increment of the electron injection ability as the working temperature increasing. Therefore, the CBF of devices increases with increasing working temperature. The cases of $\phi_n = \phi_p$ and $\phi_n > \phi_p$ have similar physical process.

2.2 $\mu_{0n} = \mu_{0p}$

In the case of $\mu_{0n} = \mu_{0p}$, Fig. 2 shows the relationship between working temperature and CBF value, the hole and electron concentration, and the electric field distribution in the bulk of organic layer under the conditions that $\phi_n > \phi_p$, $\phi_n = \phi_p$ and $\phi_n < \phi_p$, where the parameters used are: $\mu_{0n} = 1\times10^{-5}$ cm^2 • V^{-1} • s^{-1}, $\mu_{0p} = 1\times10^{-6}$ cm^2 • V^{-1} • s^{-1}, $n_0 = p_0 = 1\times10^{21}$ cm^{-3}, $F_{n0} = F_{p0} = 5\times10^5$ V • cm^{-1}, $T = 300$ K, $V = 12$ V, $d = 100$ nm, $E_g = 3.0$ eV, $N_0 = 1\times10^{21}$, $l_n = l_p = 3.0$, $\varepsilon_r = 3$.

In the cases of $\phi_n = \phi_p$, Fig. 2(a) shows that devices have the largest CBF value compared with when $\phi_n > \phi_p$ and $\phi_n < \phi_p$ in the entire region of the working temperature. Fig. 2(c) shows that the electric field intensity of the electrode interface for both electrode/organic interfaces is equal when $\phi_n = \phi_p$, electrons and holes have the same injection ability and mobility, which allows the carrier concentration to have a

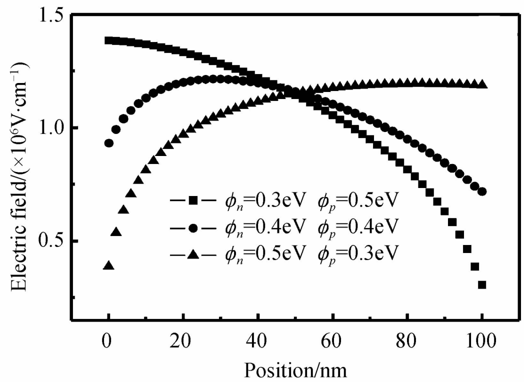

(a) The Calculated relationship between working temperature and CBF value

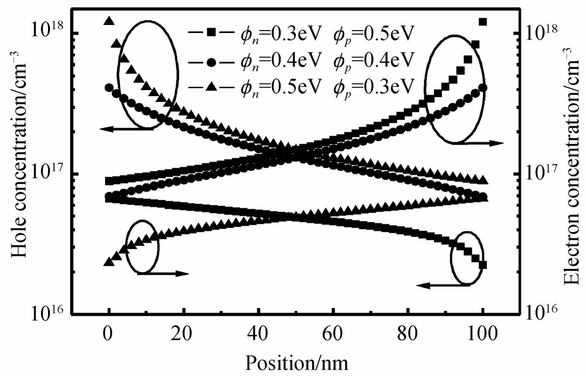

(b) The distribution of hole and electron concentration in bulk of device

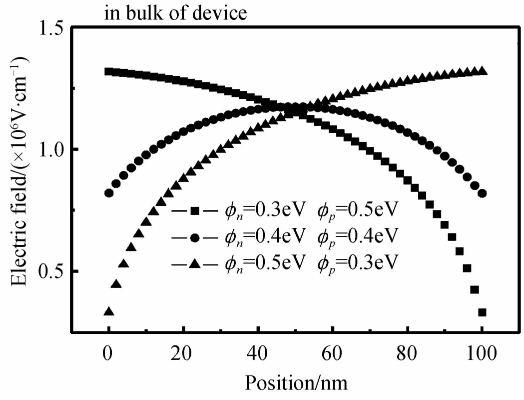

(c) The distribution of electric field intensity in the bulk of device

Fig. 2 The calculated results in the case of $\mu_{0n} = \mu_{0p}$

symmetrical distribution characteristic (as seen in Fig. 2(b)). Therefore, the device can achieve the largest CBF value. However, when $\phi_n \neq \phi_p$, the hole and electron injection ability will be different according to Eqs. (14), (19) and (20) in Ref.[17], so the CBF of the device will be decreased compared with the that when $\phi_n = \phi_p$. At the same time, the CBF value increases with increasing working temperature, similar to that when $\mu_{0n} > \mu_{0p}$, as mentioned previously.

2.3 $\mu_{0n} < \mu_{0p}$

In the case of $\mu_{0n} < \mu_{0p}$, Fig. 3 shows the relationship between working temperature and CBF value, the hole and the electron concentration distribution in the bulk of organic layer, and the electric field intensity under the condition that $\phi_n > \phi_p$, $\phi_n = \phi_p$, and $\phi_n < \phi_p$, where the parameters used in simulation are: $\mu_{0n} = 1\times10^{-5}$ cm^2 • V^{-1} • s^{-1}, $\mu_{0p} = 1\times10^{-6}$ cm^2 • V^{-1} • s^{-1}, $n_0 = p_0 = 1\times10^{21}$ cm^{-3}, $F_{n0} = F_{p0} = 5\times10^5$ V • cm^{-1}, $T = 300$ K, $V = 12$ V, $d = 100$ nm, $E_g = 3.0$ eV, $N_0 = 1\times10^{21}$, $l_n = l_p = 3.0$, $\varepsilon_r = 3$.

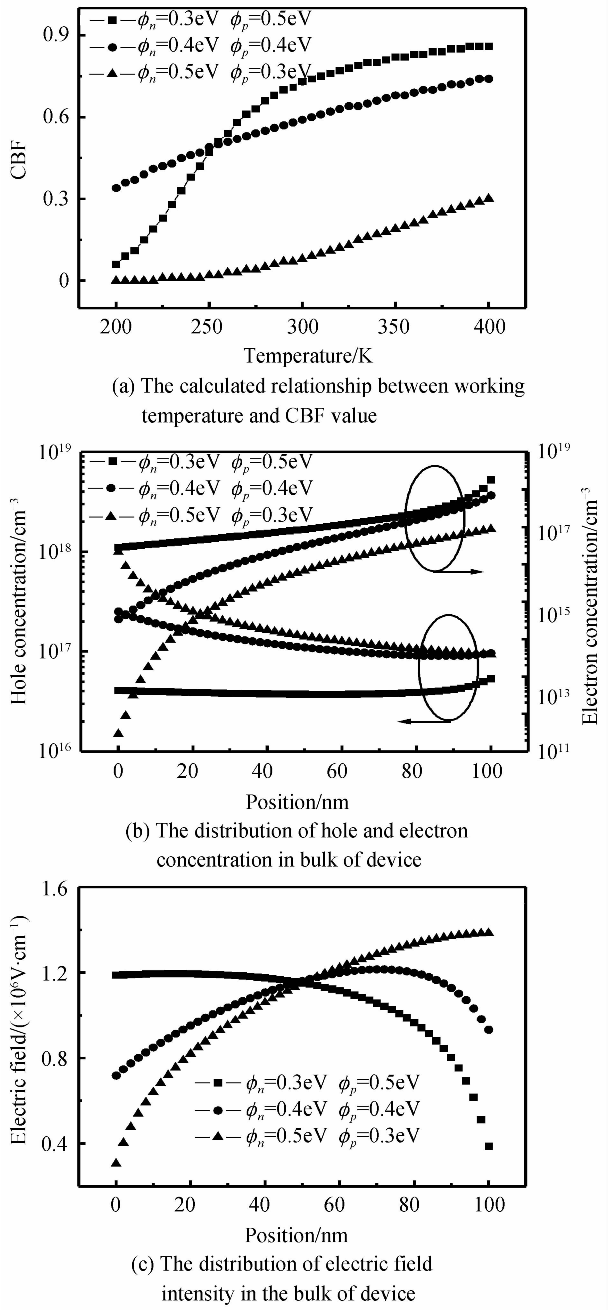

(a) The calculated relationship between working temperature and CBF value

(b) The distribution of hole and electron concentration in bulk of device

(c) The distribution of electric field intensity in the bulk of device

Fig. 3 The calculated results in the case of $\mu_{0n} < \mu_{0p}$

Fig. 3(a) shows that devices can achieve the largest CBF value when $\phi_n = \phi_p$ in the lower working temperature region, and can achieve the largest CBF value in the case of $\phi_n < \phi_p$ in the higher working temperature region. The CBF value increases as the working temperature increases, similar to the case when $\mu_{0n} > \mu_{0p}$.

3 Conclusion

In summary, the influence of working temperature on the CBF value of single layer OLEDs was studied based on the numerical model of a bipolar single layer OLED with organic level traps. The results showed that the largest CBF can be achieved when $\phi_n = \phi_n$ in the lower working temperature region no matter $\mu_{0n} >$, $=$ and $< \mu_{0p}$. In the higher working temperature region, the largest CBF can be achieved in the case of $\phi_n > \phi_p$ under the condition of $\mu_{0n} > \mu_{0p}$, with the result being the reverse in the case of $\mu_{0n} < \mu_{0p}$. When $\mu_{0n} = \mu_{0p}$, the largest CBF can be achieved in the case of $\phi_n = \phi_p$ in the entire region of the working temperature. In addition, the CBF value of the device increases with increasing working temperature.

References

[1] YANG Hui-shan, WU Li-shuang, PAN Yu-zhuo. Combined with DPVBi excton block-layer to fabricate and study on optical and electronic performance of the sub-monolayer OLED[J]. *Acta Photonica Sinica*, 2013, **42**(7): 772-776.

[2] WANG Jin, XIAO Xin-ming, ZHANG Bing, *et al*. Highly efficient tandem P-i-N white organic light emitting diode based on a new charge general layer[J]. *Acta Photonica Sinica*, 2013, **42**(2): 144-149.

[3] CUI Guo-yu, LI Chuan-nan, LI Tao, *et al*. Organic light-emitting device with Li_3N n-type doped electron injecting layer [J]. *Acta Photonica Sinica*, 2011, **40**(2): 194-198.

[4] YAMBEM S D, ULLAH M, TANDY K, *et al*. ITO-free top emitting organic light emitting diodes with enhanced light out-coupling[J]. *Laser & Photonics Reviews*, 2014, **8**(1): 165-171.

[5] LUO J X, XIAO L X, GANG Q H. Highly efficient organic light emitting devices with insulator MnO as an electron injecting and transporting material [J]. *Applied Physics Letters*, 2008, **93**: 133301-133303.

[6] HUNG L S, TANG C W, MASON M G. Enhanced electron injection in organic electroluminescence devices using an Al/LiF electrode[J]. *Applied Physics Letters*, 1997, **70**(2): 152-154.

[7] LI F, TANG H, ANDEREGG J. Fabrication and electroluminescence of double-layered organic light-emitting diodes with the Al_2O_3/Al cathode [J]. *Applied Physics*

Letters, 1997, **70**(10): 1233-1235.

[8] ZHANG X W, XU J W, XU H R, *et al*. Improving electron injection and microcavity effect for constructing highly efficient inverted top-emitting organic light-emitting diode[J]. *Optics and Laser Technology*, 2013, **45**: 181-184.

[9] TADAYYON S M, GRANDIN H M, GRIFFITHS K, *et al*. CuPc buffer layer role in OLED performance: a study of the interfacial band energies[J]. *Organic Electron*, 2004, **5**: 157-166.

[10] YOU H, DAI Y, ZHANG Z, *et al*. Improved performances of organic light-emitting diodes with metal oxide as anode buffer[J]. *Journal of Applied Physics*, 2007, **101**(2): 026105- 026105.

[11] MALLIARAS G G, SALEM J R, BROCK P J, *et al*. Electrical characteristics and efficiency of single-layer organic light-emitting diodes[J]. *Physical Review B*, 1998, **58**(20): R13411-R13414.

[12] CHAN I M, HONG F C. Improved performance of the single-layer and double-layer organic light emitting diodes by nickel oxide coated indium tin oxide anode[J]. *Thin Solid Films*, 2004, **450**(2): 304-311.

[13] MARKHAM J P J, LO S C, MAGENNIS S W, *et al*. High-efficiency green phosphorescence from spin-coated single-layer dendrimer light-emitting diodes[J]. *Applied Physics Letters*, 2002, **80**(15): 2645-2647.

[14] LU F P, LIU X B, XING Y Z. Numerical study of the influence of applied voltage on the current balance factor of single layer organic light-emitting diodes[J]. *Journal of Applied Physics*, 2014, **115**(16): 164508.

[15] MEYER H, HAARER D, NAARMANN H, *et al*. Trap distribution for charge carriers in poly (paraphenylene vinylene)(PPV) and its substituted derivative DPOP-PPV [J]. *Physical Review B*, 1995, **52**: 2587-2898.

[16] KAŽUKAUSKAS V, TZENG H, CHEN S A. Trap levels and effect of oxygen in poly [2-methoxy-5-(2′-ethyl-hexyloxy)-1, 4-phenylene vinylene] diodes[J]. *Applied Physics Letters*, 2002, **80**(11): 2017-2019.

[17] SHEN J, YANG J. Physical mechanisms in double-carrier trap-charge limited transport processes in organic electroluminescent devices: a numerical study[J]. *Journal of Applied Physics*, 1998, **83**(12): 7706-7714.

[18] BLOM P W M, DE JONG M J M, VLEGGAAR J J M. Electron and hole transport in poly(pphenylene vinylene) devices[J]. *Applied Physics Letters*, 1996, **68**(23): 3308-3310.

[19] PRNG Y Q, ZHANG F J, LI H R, *et al*. Numerical study of distribution of electric field and carrier concentration in luminescent layer of organic light emitting devices[J]. *Journal of Semiconductors*, 2003, **24**(3): 274-278.

[20] GUMMEL H K. A self-consistent iterative scheme for one-dimensional steady state transistor Calculations[J]. *IEEE Transactions on Electron Devices*, 1934, **11**(10): 455-465.

[21] SCHARFETTER D L, GUMMEL H K. Large-signal analysis of a silicon read diode scillator[J]. *IEEE Transactions on Electron Devices*, 1969, **16**(1): 64-77.